

# Ablation Study in a Capillary Sustained Discharge

Michael Keidar and Iain D. Boyd

Department of Aerospace Engineering/University of Michigan

Anthony Williams and Richard Beyer

Army Research Laboratory

Abstract- Electrothermal-chemical (ETC) ignition systems have been demonstrated in gun systems to provide desirable characteristics including reproducible shorter ignition delays. The optimum combination of capillary tube and fuse wire properties has not been identified yet. We present a combined theoretical and experimental study of the capillary discharge with an aim to develop a capillary plasma source with efficient energy conversion. The major emphasis in the present capillary discharge model is the ablation phenomenon. Consideration is given to different characteristic sub-regions near the ablated surface: namely, a space-charge sheath, a Knudsen layer, and a hydrodynamic layer. A kinetic approach is used to determine the parameters at the interface between the kinetic Knudsen layer and the hydrodynamic layer. Coupling the solution of the non-equilibrium Knudsen layer with the hydrodynamic layer provides a self-consistent solution for the ablation rate. According to the model predictions, the peak electron temperature is about 1.4 eV, the polyethylene surface temperature is about 700 K, and the pressure is about 10 MPa in the case of a 0.6 kJ discharge. In parallel, a parametric experimental study of the capillary ablation process is conducted. The ablation rates are measured for capillary tubes made of polyethylene and Teflon. Both experimental measurements and simulations indicate that the ablated mass increases with the peak discharge current and that a smaller diameter capillary yields a larger ablated mass. It is found that model predictions agree well with experimental measurements.

## Report Documentation Page

*Form Approved*  
*OMB No. 0704-0188*

Public reporting burden for the collection of information is estimated to average 1 hour per response, including the time for reviewing instructions, searching existing data sources, gathering and maintaining the data needed, and completing and reviewing the collection of information. Send comments regarding this burden estimate or any other aspect of this collection of information, including suggestions for reducing this burden, to Washington Headquarters Services, Directorate for Information Operations and Reports, 1215 Jefferson Davis Highway, Suite 1204, Arlington VA 22202-4302. Respondents should be aware that notwithstanding any other provision of law, no person shall be subject to a penalty for failing to comply with a collection of information if it does not display a currently valid OMB control number.

1. REPORT DATE <b>2006</b>	2. REPORT TYPE	3. DATES COVERED <b>00-00-2006 to 00-00-2006</b>	
4. TITLE AND SUBTITLE <b>Ablation Study in a Capillary Sustained Discharge</b>		5a. CONTRACT NUMBER	
		5b. GRANT NUMBER	
		5c. PROGRAM ELEMENT NUMBER	
6. AUTHOR(S)		5d. PROJECT NUMBER	
		5e. TASK NUMBER	
		5f. WORK UNIT NUMBER	
7. PERFORMING ORGANIZATION NAME(S) AND ADDRESS(ES) <b>University of Michigan, Department of Aerospace Engineering, 1301 Beal Avenue, Ann Arbor, MI, 48109</b>		8. PERFORMING ORGANIZATION REPORT NUMBER	
9. SPONSORING/MONITORING AGENCY NAME(S) AND ADDRESS(ES)		10. SPONSOR/MONITOR'S ACRONYM(S)	
		11. SPONSOR/MONITOR'S REPORT NUMBER(S)	
12. DISTRIBUTION/AVAILABILITY STATEMENT <b>Approved for public release; distribution unlimited</b>			
13. SUPPLEMENTARY NOTES <b>Presented at the 13th International Symposium on Electromagnetic Launch Technology (EML), Held May 22 - 25, 2006 in Potsdam, Brandenburg, Germany Copyright 2006 IEEE. Published in the Proceedings, <a href="http://emlsymposium.org/archive.html#">http://emlsymposium.org/archive.html#</a></b>			
14. ABSTRACT			
15. SUBJECT TERMS			
16. SECURITY CLASSIFICATION OF:			17. LIMITATION OF ABSTRACT
a. REPORT <b>unclassified</b>	b. ABSTRACT <b>unclassified</b>	c. THIS PAGE <b>unclassified</b>	<b>Same as Report (SAR)</b>
			18. NUMBER OF PAGES <b>10</b>
			19a. NAME OF RESPONSIBLE PERSON

## I. INTRODUCTION

Electrothermal-chemical (ETC) guns are designed to introduce electrical energy into the chamber of a conventional chemical gun system.<sup>1</sup> An ETC gun has the potential to improve the performance of conventional guns by enhancing the ignition and combustion characteristics of propellants. One of the significant advantages of the ETC system is a smaller ignition delay time as compared with conventional igniters. Typically, ETC ignition delay is of the order of 1-2 ms while advanced conventional igniters have been shown to exhibit 6-8 ms ignition delay.<sup>1</sup> An ETC system has two components, namely a plasma source and a chemical propellant system. In this system, the propellant is usually ignited with plasma introduced by a jet from a capillary discharge or by an arc from an exploding wire inside the propellant charge.<sup>1,2,3</sup> Several plasma properties are important for this application. The temperature of the plasma is about 10,000 K. Significant radiation from the plasma leads to photochemical changes within the propellant surface and in-depth structure. The presence of the various ion and neutral species may lead to chemical reaction at the propellant surface. In addition, the highly-directed velocity of the plasma jet affects the heat transfer. All of the above plasma-propellant interactions are dependent on the plasma properties that are determined by the plasma source. Therefore, accurate prediction of plasma properties from the capillary discharge is important for understanding plasma-propellant interactions. The main physical processes occur in the capillary in a similar way to an ablation-controlled discharge.

Significant efforts have been applied to model the ablation-controlled discharge that is commonly used as a plasma source for ETC.<sup>4,5,6</sup> Some initial theoretical models aimed to analyze existing experimental data and build a phenomenological description of the ablation processes. Later, more sophisticated steady state<sup>7,8</sup> and unsteady theoretical models<sup>9,10,11</sup> were proposed to describe capillary discharges for an electrothermal gun. However, these models are based on various assumptions about the ablation rate. In most models, the ablation rate is determined somewhat arbitrarily or adjusted to fit the measured total ablated mass. It was, however, shown recently that material ablation into the discharge plasma is a rather complicated phenomenon.<sup>12,13</sup> For instance, the same ablation rate can correspond to very different discharge conditions. A self-consistent model of the capillary discharge that takes into account ablation kinetics was developed.<sup>14,15</sup> The model is based on a kinetic description of the Knudsen layer and a hydrodynamic description of the collision-dominated plasma region. In this paper, we present a capillary model for an ETC that includes self-consistent consideration of the ablation phenomena. In addition we present experimental measurements of the capillary ablation mass for various discharge conditions and capillary geometry. We compare our model predictions with measured data in an effort to validate the overall capillary discharge model.

## II. EXPERIMENTAL SET-UP

Figures 1 and 2 illustrate the experimental fixture utilized in the present work. A 25.4-mm (1-inch) diameter outer insulator contains a 6.4-mm diameter hole which houses a variable length capillary tube and inner insulator. Both 30-mm and 38-mm long capillary tubes are investigated. The capillary tube outer diameters are fixed at 6.2-mm,

however, two different inner diameters (3.18-mm and 4.32-mm) are considered. The two different capillary tube lengths are accommodated by adjusting the total length of the anode (brass rod + carbon disk) and the supporting inner insulator (see Figs 1,2.). The capillary nozzle is made of tantalum/tungsten and has the following dimensions: length = 11-mm, OD = 6.2-mm, ID = 4.4-mm. The nozzle serves as the cathode which is electrically connected to the anode by a 0.10-mm (0.004-inch) diameter aluminum fuse wire. The mass of the aluminum fuse wire is 0.6 mg and 1.0 mg for the 23-mm and 38-mm capillary tubes, respectively.

The capillary-sustained plasma characteristics observed are produced by an electrical discharge directed across the aluminum fuse wire. The system, which delivers the current across the fuse wire, includes a standard pulse forming network (PFN) power supply. The PFN power supply is used to charge a 1700  $\mu\text{F}$  capacitor. The system charging voltage ranges from 680 V to 1210 V with corresponding stored energies of 370 J to 650 J in the experiments discussed here. The current is delivered across the fuse wire producing the electrically charged plasma. For this system, the resulting plasma pulse width is typically around 385  $\mu\text{s}$ . The discharge current is measured by integrating the output of a Rigowski coil and high voltage probes are used to measure the voltage across the electrodes. The carbon disk portion of the anode is introduced specifically because it has been shown to have minimal erosion (compared to other materials) characteristics in the plasma environment. Thus, the carbon disk has minimal contribution to the nearby capillary sustained plasma. Once the plasma is formed inside the capillary tube, the local pressure begins to rise and the plasma vents through the nozzle into open-air. The plasma is temporarily sustained and enhanced by ablating material from the capillary wall. The nozzle mass is also recorded before and after each experiment.

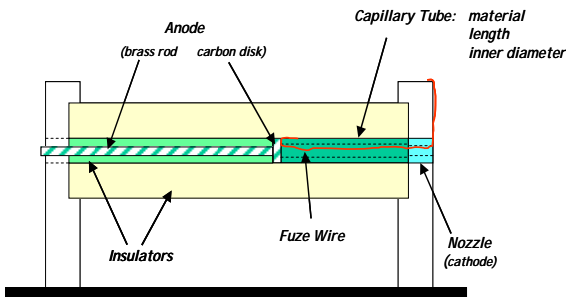


Figure 1. Schematic of Experimental Setup

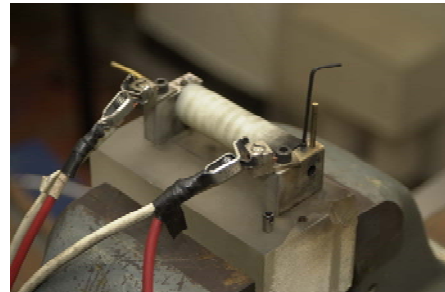
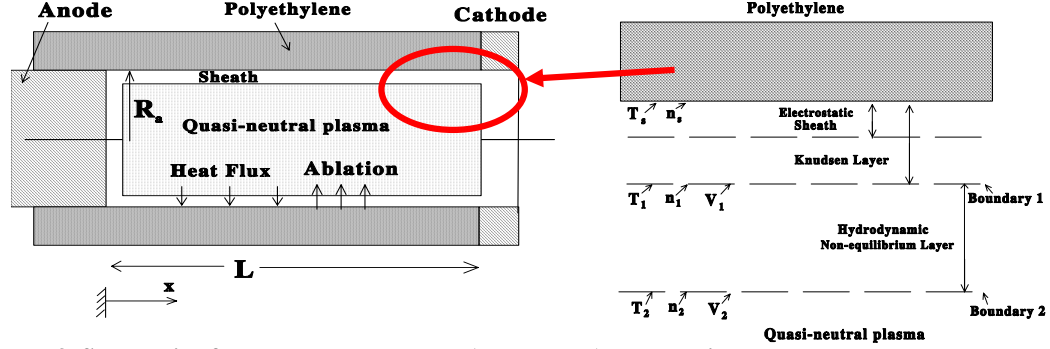


Figure 2. Photograph of Experimental Setup

### III. THE ABLATION-CONTROLLED DISCHARGE MODEL

In this section, the model is described for the plasma generation processes (ablation, heating, radiation, ionization etc.) and plasma acceleration along a capillary of a pulsed electrical discharge. Figure 3 shows some characteristic regions in the interface between the discharge plasma and the dielectric wall such as an electrical sheath near the dielectric, the Knudsen and hydrodynamic layers, and a quasi-neutral plasma. Different kinetic and hydrodynamic phenomena determine the main features of the plasma flow including Joule heating, radiative and convective heat transfer to the dielectric, and electrothermal acceleration of the plasma up to the sound speed at the cavity exit. The

central region is the quasi-neutral plasma that occupies almost the entire capillary since typically the transition region scale length is much smaller than the capillary radius. The plasma region is separated from the dielectric surface by the vapor layers (Knudsen layer and hydrodynamic layer). Finally, the plasma-wall transition region includes the electrostatic sheath attached to the wall.



**Figure 3. Schematic of the problem geometry (not to scale) and multi-layer structure near the ablated surface.**

The plasma is heated due to electric current flowing through the capillary. The energy transfer from the plasma column to the capillary wall consists of the heat transfer by particle fluxes and radiation heat transfer. Energy is absorbed by the capillary walls and dissipated by thermal conductivity and material evaporation. Ablated flux builds up a vapor layer in the vicinity of the wall. Under the considered conditions the mass, momentum and energy conservation equations have the following forms:

$$A \left( \frac{\partial \rho}{\partial t} + \frac{\partial \rho V}{\partial x} \right) = 2\pi R_a \Gamma(t, x) \quad (1)$$

$$\rho \left( \frac{\partial V}{\partial t} + V \frac{\partial V}{\partial x} \right) = -\frac{\partial P}{\partial x} \quad (2)$$

$$\rho \left( \frac{\partial \varepsilon}{\partial t} + V \frac{\partial \varepsilon}{\partial x} \right) = -P \frac{\partial V}{\partial x} + Q_j - Q_r - Q_F \quad (3)$$

where  $\varepsilon = \frac{3}{2} \frac{T_p}{m} + \frac{V^2}{2}$ . The radiation energy flux  $Q_r$  includes the radiation for a continuum spectrum based on a theoretical model<sup>16</sup>. According to Ref. 17, the radiation in continuum from a carbon plasma in the considered parameter range provides the main contribution. In addition, a black-body radiation from the plasma will be considered and compared with other energy sources and sinks. The particle convection flux  $Q_F$  includes energy associated with electron and ion fluxes to the dielectric wall that leads to plasma cooling. Radiation and convection heat fluxes from the plasma to the cavity wall (see Fig. 3) determine the thermal regime of the capillary walls. The temperature inside the dielectric can be calculated from the heat transfer equation:

$$\frac{\partial T}{\partial t} = a \frac{\partial^2 T}{\partial r^2} \quad (4)$$

where  $a$  is the thermal diffusivity. Having calculated the plasma density and electron temperature (Eqs. 1-3) one can calculate the chemical plasma composition considering Local Thermodynamic Equilibrium (LTE) in the way described previously<sup>18,19</sup>. In the considered range of electron temperature (1-2 eV) and plasma density ( $10^{24}$ - $10^{26}$  m<sup>-3</sup>) it is assumed that polyatomic molecules C<sub>2</sub>H<sub>4</sub> are fully dissociated and we will start our

consideration from the point when we have a gas containing atoms of C and H. The distribution of the atoms, multiply ionized ions, and electrons obeys the corresponding Saha equation. Knowing the plasma pressure and temperature, ionization potential, and partition functions for  $z$ -fold ionization processes allows calculation of the atom and ion species density. The Saha equations should be supplemented by the conservation of nuclei and quasi-neutrality in order to calculate plasma composition. Plasma may depart from the ideal state under the considered high-density conditions. Due to non-ideal plasma effects, corrections are considered to the ionization energies, partition functions and plasma pressure.<sup>20</sup> The capillary wall ablation is modeled in the framework of the previously developed kinetic model.<sup>12,13</sup> Two different layers between the ablated surface and the plasma bulk are considered as shown in Fig. 3: (i) a kinetic non-equilibrium layer adjacent to the surface with a thickness of about one mean free path; and (ii) a collision-dominated layer with thermal and ionization non-equilibrium. The plasma-wall transition layer includes also an electrical sheath described below. Solving the conservation equations in the hydrodynamic layer<sup>12,13</sup> the ablation rate has the following form:

$$\Gamma = mV_1 n_1 = mn_1 \sqrt{\frac{1}{m} \cdot \frac{(kn_2 T_2 - kn_1 T_1)}{(n_1 - \frac{n_1^2}{n_2})}} \quad (5)$$

It should be noted that this equation has a real solution if the following conditions are fulfilled:  $kT_2 n_2 < kT_1 n_1$  and  $n_1 > n_2$ ; otherwise, the solution of equation 5 breaks down. Physically, this means that backflux is much higher than the primary flux. Therefore, in this case, deposition on the dielectric surface takes place instead of ablation. The system of equations is closed if the equilibrium vapor pressure can be specified that determines parameters ( $n_s$  and  $T_s$ ) at the dielectric surface. Various models and an experiment<sup>21</sup> show that the vapor pressure for polyethylene can be approximated as follows:

$$P = \exp\left(A \cdot \left[\frac{1}{B} - \frac{1}{T}\right]\right) \quad \dots\dots\dots (6)$$

where  $A=3759$ ;  $B=453$ , and  $T$  is in K. Near the dielectric surface in the capillary, an electrostatic sheath is formed to maintain the floating potential on the wall with respect to the plasma. The potential drop of the electrostatic sheath near the dielectric wall is negative in order to repel the excess thermal electrons, so that the random electron current density  $j_{eth}$  is equal to the ion current density  $j_i$ .

#### IV. RESULTS

The electron temperature distribution during the discharge is shown in Fig. 4. For reference, the experimentally measured current waveform adopted in the simulations is also shown. It can be seen that the electron temperature temporal distribution follows the current waveform. The temperature peaks at 1.4 eV and then decreases towards the end of the pulse.

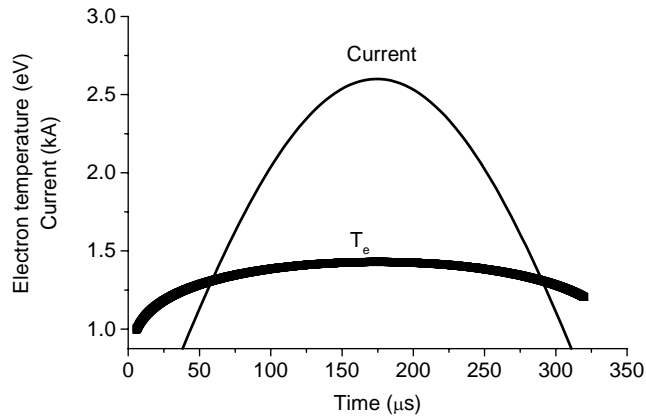


**Figure 4. Temporal variation of the electron temperature and current waveform used in the simulations.**

The axial and temporal distribution of total pressure is shown in Fig. 5. It can be seen that pressure peaks at about 10 MPa and then decreases towards the end of the pulse to about 1 MPa. Spatial and temporal distributions of the different species are shown in Fig. 6. All species densities peak at about 150-200  $\mu\text{s}$ . One can see that the neutral density is much higher than the ion density, thus indicating that the ionization degree is small (approximately 10-20 % for the main portion of the pulse).

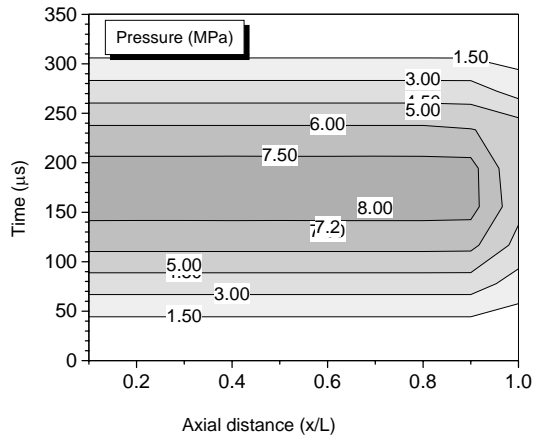


**Figure 5. Temporal and spatial variation of the pressure in the capillary.**

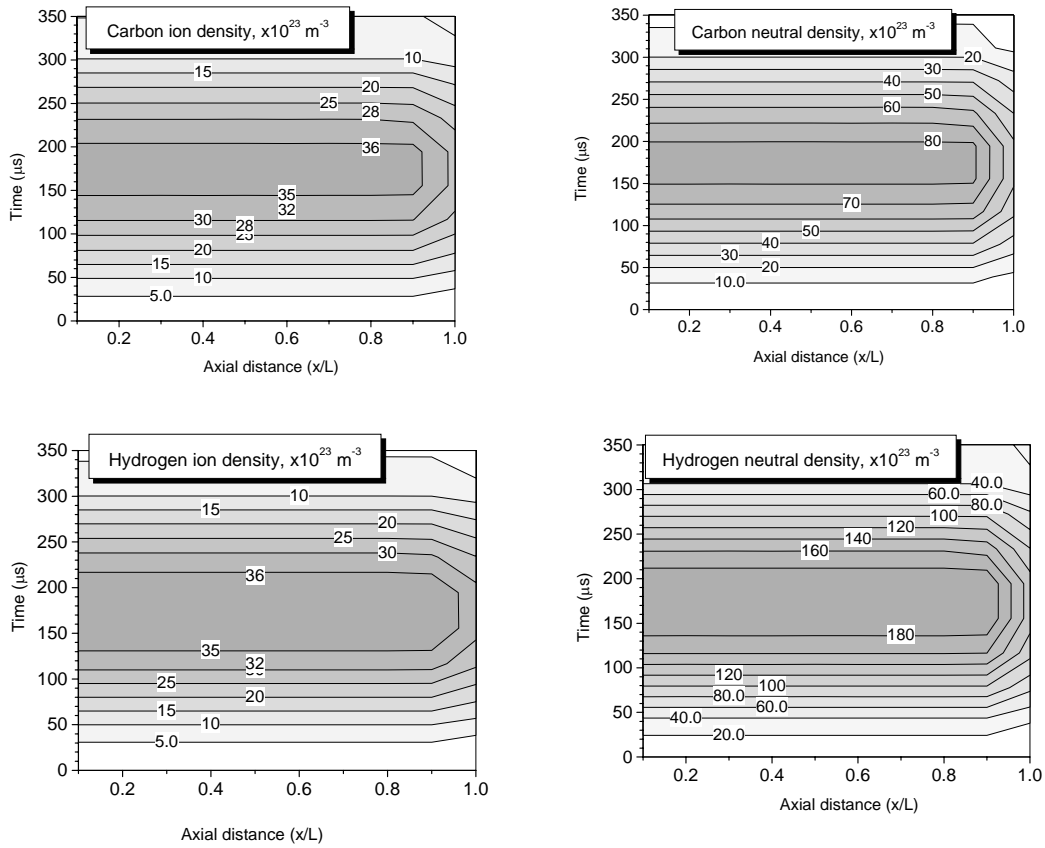


**Figure 6. Temporal and spatial variation of the chemical species during discharge pulse.**

The surface temperature distribution is shown in Fig. 7. The surface temperature sharply increases initially and peaks at about 700 K. Only slight variation of the surface temperature along the capillary is found in accordance with previous predictions.

Capillary geometry determines the ablation process in the capillary by affecting the mass and energy balance. The dependence of the ablated mass on the peak discharge current is shown in Fig. 8. The ablated mass has a linear dependence on the discharge peak current. For comparison, experimental data are also shown in Fig. 8. It can be seen that both simulations and experiment suggest that the ablated mass increases as the capillary inner diameter decreases. This effect is explained by increased current density in the capillary, which affects the ablation rate through Joule heating. Reasonable agreement is obtained although the predicted ablated mass is lower than that measured in the experiments. It should be pointed out that above calculations were performed assuming that returned atoms and ions do not form film at the polyethylene surface. On the other hand it can be considered that only carbon atom and carbon ion deposition takes place, as the hydrogen atoms and ions will be re-evaporated<sup>15</sup>. The last assumption is supported by previous studies of dielectric (Teflon) ablation into C-F plasmas indicated that dielectric can be significantly carbonized (charred) dependent on operational conditions.<sup>22</sup> In this paper we also study parametrically effect of the condensation at the dielectric surface. We introduce a new parameter,  $v$ , which is the

fraction of the backflux that condense at the surface. In the case  $\nu=1$  all particles returning to the surface will condense, while small parameter  $\nu$  means that only a fraction of the backflux form the film. Dependence of the ablated mass on this parameter is shown in Fig.9. One can see the best agreement with experimental data is achieved if  $\nu=0.6-0.7$ .

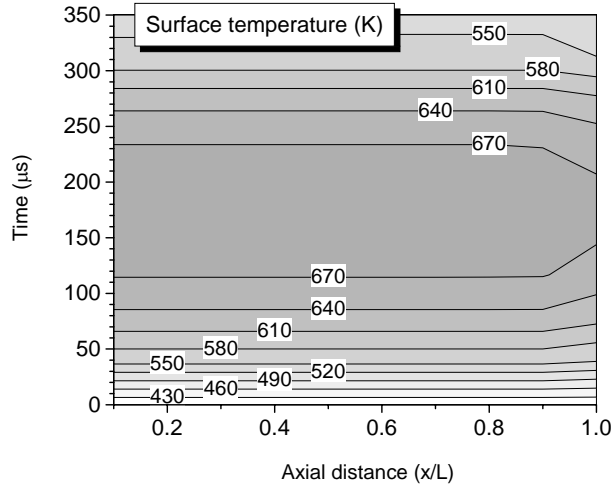


Figure 7. Temporal and spatial variation of the polyethylene surface temperature.

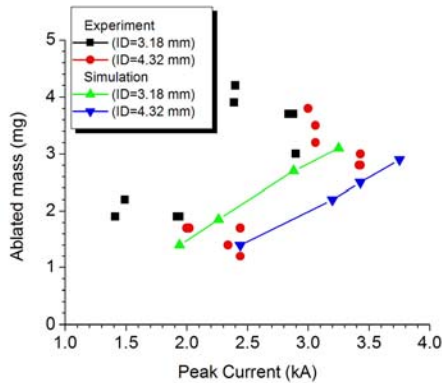


Figure 8. Dependence of the ablated mass (polyethylene) on the peak discharge current. Comparison experiment and simulations.

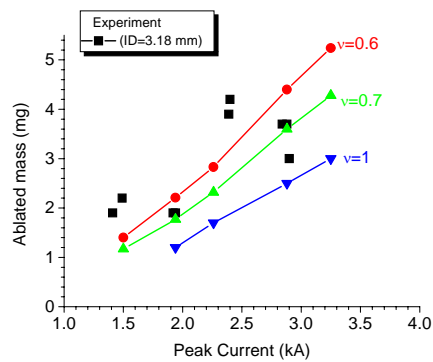


Figure 9. Dependence of the ablated mass (polyethylene) on the peak discharge current with deposition fraction as a parameter. Comparison experiment and simulations.

#### IV. CONCLUDING REMARKS

Self-consistent analysis of the different characteristic regions near the ablated surface allows determination of the rate of ablation without employing various assumptions used previously. For instance, in the present analysis it is not necessary to assume the energy fraction causing capillary wall ablation. Both experimental measurements and simulations indicated that the ablation rate increased nearly linearly with discharge peak

current. In addition, it was found that the ablated mass increased with a decrease in capillary radius. The effect of the ablated mass dependence on the current density in the capillary can be explained by invoking the fact that the main heat source inside the capillary is the Joule heat that depends on the current density. Generally, good agreement was found between model predictions and experimental measurements.

### *Acknowledgment*

The authors gratefully acknowledge the financial support by the Army Research Office, Grant No. W911NF-04-1-0251 (Dr. Kevin McNesby, technical monitor). The authors thank Dr. Michael Nusca from the Army Research Laboratory for very useful discussions and suggestions.

---

### *References*

- [1] A. Koleczko, W. Ehrhard, S. Kelzenberg and N. Eisenreich, "Plasma Ignition and Combustion", Prop. Explos. Pyrotech., vol. 26 pp.75-83, 2001.
- [2] A. Birk, M.D. Guercio, A. Kinkennon, D.E. Kooker, and P. Kaste, "Interrupted-burning tests of plasma-ignited JA2 and M30 grains in a closed chamber", Prop. Explos. Pyrotech., vol. 25 pp.133-142, 2000.
- [3] J. Li, T.A. Litzinger and S. T. Thynell, "Plasma Ignition and Combustion of JA2 Propellant", J. Prop. Power, vol. 21 pp.44-53, Feb, 2005.
- [4] J.D. Powell and A.E. Zielenski, "Capillary discharge in the electrothermal gun", IEEE Trans. Magnetics, vol. 29 p. 591-596, Jan, 1993.
- [5] D. Zoler and R. Alimi, "A proof of the need for consistent treatment in modeling of capillary ablative discharges", J. Phys. D: Appl. Phys., vol. 28 pp. 1141-1152, 1995.
- [6] M. R. Zaghoul, M.A. Bourham and J.M. Doster, "Semi-analytical modeling and simulation of the evolution and flow of Ohmically-heated non-ideal plasmas in electrothermal guns", J. Phys. D: Appl. Phys., vol. 34, pp.772-786, 2000.
- [7] P. Kovitya and J. J. Lowke, "Theoretical predictions of ablation-stabilized arcs confined in cylindrical tubes", J. Phys. D: Appl. Phys., vol. 17, pp. 1197-1212, 1984.
- [8] C. B. Ruchti and L. Niemeyer, "Ablation controlled arc", IEEE Trans. Plasma Sci., vol. 14 pp. 423-434, 1986.
- [9] A. Loeb and Z. Kaplan, "A Theoretical model for the physical process in the confined high-pressure discharge of electrothermal launchers", IEEE Trans. Magnetics, vol. 25, pp. 342-346, Jan 1989.
- <sup>10</sup> R.B. Mohanti, J.G. Gilligan, and M.A. Bourham, "Time-dependent simulation of weakly nonideal plasmas in electrothermal launchers", Phys. Fluids. B, vol. 3 (11), pp. 3046-3052, Nov 1991.

- 
- [11] K. Kim, IEEE Trans. Plasma Sci., "Time-dependent one-dimensional modeling of pulsed plasma discharge in a capillary plasma device", vol. 31, pp.729-735, Aug 2003.
- [12] M. Keidar, J. Fan. I.D. Boyd and I.I. Beilis, "Vaporization of Heated Materials into Discharge Plasmas", Journal of Applied Physics, vol. 89, pp. 3095-3098, 2001.
- [13] M. Keidar, I.D. Boyd and I.I. Beilis, "On the model of Teflon ablation in an ablation-controlled discharge", J. Phys. D: Appl. Phys., vol. 34 pp.1675-1677, 2001.
- [14] M. Keidar, I.D. Boyd and I.I. Beilis, "Model of an Electrothermal Pulsed Plasma Thruster", Journal Propulsion & Power, vol. 19, No. 3, pp. 424-430, 2003.
- [15] M. Keidar and I. D. Boyd, "Ablation study in the capillary discharge of an electrothermal gun," Journal of Applied Physics, vol. 99, 053301, 2006.
- [16] G. I. Kozlov, V. A. Kuznetsov, and V. A. Masyukov, "Radiative Losses by Argon Plasma and the Emissive Model of a Continuous Optical Discharge", Sov. Phys. JETP, vol. 39, pp.463-468, 1974.
- [17] A. I. Zemskov, V. V. Prut, and V. A. Khrabrov, "Pulsed Discharge in Dielectric Chamber", Sov. Phys. Tech. Phys., vol. 17, pp. 285-289, 1972.
- [18] P. Kovitya, "Thermodynamic and Transport Properties of Ablated Vapors of PTFE, Alumina, Perspex and PVC in the Temperature range 5000-30000 K, IEEE Transaction on Plasma Science, vol. 12, pp. 38-42, 1984.
- [19] C.S. Schmahl and P.J. Turchi, "Development of Equation-of-State and Transport Properties for Molecular Plasmas in Pulsed Plasma Thrusters. Part I: A Two-Temperature Equation of State for Teflon", Proceeding of the International Electric Propulsion Conference, vol. 1, (The Electric Propulsion Society, Worthington OH), p. 781, 1997.
- [20] K. Gunther and R. Radke, Electrical properties of weakly non-ideal plasmas (Boston, Birhauser, 1984)
- [21] Beaton C.F. and Hewitt G.F. Physical Property data for design engineer, Hemisphere publishing Corp., New York, 1989
- [22] M. Keidar, I.D. Boyd, E. Antonsen, F. Gulchinski, G.G. Spanjers, "Propellant charring in pulsed plasma thrusters", J. Prop. Power, vol. 20, pp. 978-984, Nov. 2004.